Magnetic flux tube tunneling

R. B. Dahlburg
Code 6440, Naval Research Laboratory, Washington, DC 20375-5344

S. K. Antiochos
Code 7675, Naval Research Laboratory, Washington, DC 20375-5352

D. Norton
SAIC, 550 Camino el Estero, Suite 205, Monterey, California 93943
(Received 29 May 1996; revised manuscript received 19 March 1997)

We present numerical simulations of the collision and subsequent interaction of *orthogonal* magnetic flux tubes. The simulations were carried out using a parallelized spectral algorithm for compressible magnetohydrodynamics. It is found that, under a wide range of conditions, the flux tubes can ''tunnel'' through each other, a behavior not previously seen in studies of either vortex tube or magnetic flux tube interactions. Two conditions must be satisfied for tunneling to occur: the magnetic field must be highly twisted with a field line pitch $\gg 1$, and the Lundquist number must be somewhat large, $\geqslant 2880$. An examination of magnetic field lines suggests that tunneling is due to a double-reconnection mechanism. Initially orthogonal field lines reconnect at two specific locations, exchange interacting sections, and ''pass'' through each other. The implications of these results for solar and space plasmas are discussed. [S1063-651X(97)02008-4]

PACS number(s): 52.30.Jb, 52.55.Dy, 52.65.Kj, 95.30.Qd

INTRODUCTION

Models of magnetic reconnection in the Sun's interior and atmosphere usually begin with a purely two-dimensional geometry. However, the magnetic field at the solar photosphere is observed to be organized into isolated flux bundles [1], a structure which must continue into the corona. In addition, photospheric motions are likely to ''wind up'' this magnetic field, producing twisted flux tubes [2,3]. Interaction between twisted flux tubes has been proposed as a mechanism for coronal heating [4–6] and might be the origin of the fine-scale temporal variability of hard x-ray and microwave emission observed in two-ribbon flares [7,8]. Flux tubes also are widely believed to be the dominant magnetic structure in the convection zone [9]. Coronal mass ejections have been identified in the interplanetary medium as flux ropes [10], which are thought to be essential ingredients for reconnection at the magnetopause [11] and magnetotail [12]. Therefore, a key issue for understanding many important phenomena in solar and space physics is the nature of flux tube interaction.

We are using numerical simulations to investigate the basic physics of magnetic flux tube collision and reconnection. Our explicit, Fourier collocation algorithm, which is described in detail elsewhere [13,14], solves the three-dimensional (3D), compressible, dissipative magnetofluid equations in a dimensionless form [14]. The geometry used is that of a triply periodic cube with sides equal to 2π, making a Fourier spectral method the optimal choice for spatial discretization. The results described here were computed by a parallelized version of our code implemented on the 256 processor NRL TMC CM5E [15]. A typical resolution for the runs in this paper is 128^3 Fourier modes, requiring approximately 5 s per time step and 1.05 GB of parallel memory.

The initial conditions consist of two orthogonal flux tubes of finite radius R, and a flow field which drives them together. Each of the tubes is initialized using the Gold-Hoyle model of a uniformly twisted, cylindrical, force-free magnetic field [$\mathbf{B}=(B_x,B_y,B_z)$] [16], viz.,

$$B_x=\frac{B_0 br\,\sin\phi}{1+b^2r^2};\quad B_y=-\frac{B_0 br\,\cos\phi}{1+b^2r^2};\quad B_z=-\frac{B_0}{1+b^2r^2}, \tag{1}$$

where $B_0=4$, and r and ϕ are the radial and cylindrical coordinates of the flux tube. The parameter b measures the field line pitch, i.e., $b=d\phi/dz$. In order to maintain ideal equilibrium, the uniform gas pressure (p) outside the tube is set to $p=p_0+2B_0^2/(1+b^2R^2)$, where p_0 is the gas pressure inside the tube ($=20/3$), and R is the flux tube radius ($=11\pi/48$). To ameliorate the Gibbs phenomenon due to the Fourier series discretization of the sharp cutoff at $r=R$, we pass these initial conditions through a raised cosine filter [17]. The initial density is uniform ($\rho=1$). The values for B_0 and p_0 yield a plasma $\beta=0.42$ at the flux tube axis.

Our simulation box consists of a cube with the dimensions: $0\leqslant x\leqslant 2\pi$, $0\leqslant y\leqslant 2\pi$, $0\leqslant z\leqslant 2\pi$. This cube is shown in Fig. 1. One tube is initially horizontal with its central axis located at ($x=5\pi/4$, $z=\pi$), the other is vertical with its axis located at ($x=3\pi/4$, $y=3\pi/4$) in order to break the symmetry. [We have performed a symmetric simulation with the second flux tube centered at ($x=3\pi/4$, $y=\pi$) which also exhibits tunneling.] We note from these numbers that the flux tubes are separated initially by a finite gap of field-free plasma of width $\pi/24$.

There are four physically distinct relative orientations for the flux tubes, depending on the choice of the axial and azimuthal magnetic field in each of the tubes. In all our simu-

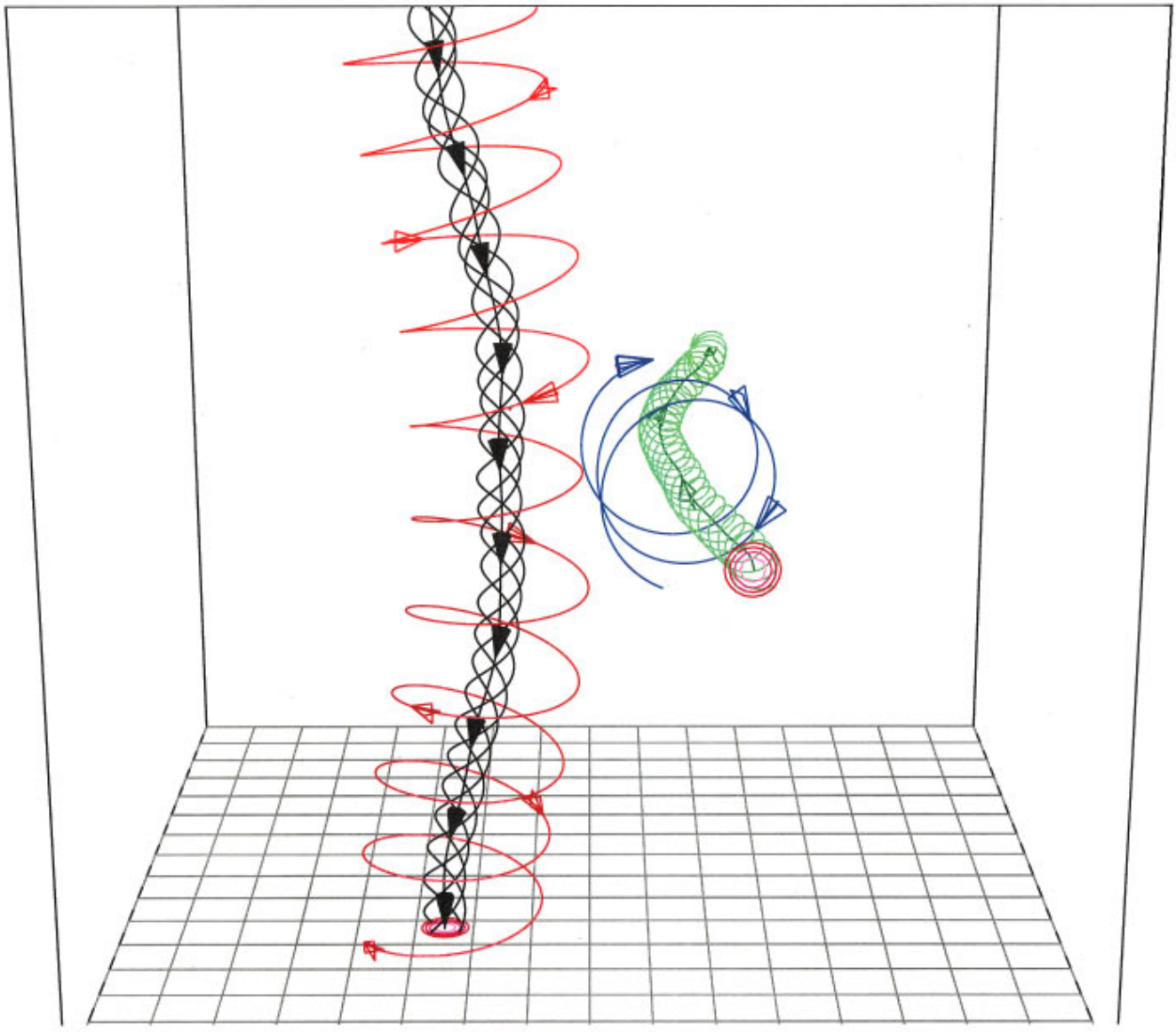

FIG. 1. (Color). Structure of the magnetic field at $t=7.8$. The simulation cube is outlined by black lines and the bottom grid (at $z=0$) is represented by the light gray lines (only every 8th grid line is plotted). The viewpoint has been chosen so that the z axis is in the vertical direction, x is to the right and y is into the figure. Note that the viewpoint is inside the simulation box, the origin (0,0,0) is located at the bottom left-hand corner slightly behind the viewer and, hence, is not visible in the figure. Five contours of $|\mathbf{B}|$ from $|\mathbf{B}|_{\max}$ to $0.75|\mathbf{B}|_{\max}$ are plotted on the plane nearest the viewer $y=0$, and on bottom grid. Five black (green) field lines indicate the central region of the vertical (horizontal) flux tube. These field lines originate from the center and the corners of a 4×4 grid-point square that is centered on the point of $|\mathbf{B}|_{\max}$. Also shown is a field line (red) at the boundary of the vertical tube and two windings of a field line (blue) at the boundary of the horizontal tube.

lations the twist and orientation are chosen so as to maximize the possibility of reconnection—the axial (azimuthal) field of the horizontal tube is directed opposite to the azimuthal (axial) field of the vertical tube in the collision region. It is evident in Fig. 1 that in the region between the flux tubes, the blue azimuthal field line of the horizontal tube is directed upwards, whereas the black axial field line of the vertical tube is directed downward. Similarly, the red azimuthal field line of the vertical tube is directed opposite to the green axial line of the horizontal tube.

The two flux tubes are driven together by an initial velocity field given by

$$\mathbf{v}(x,y,z,t=0)=A_v[-\sin x(\cos y+\cos z)\hat{\mathbf{e}}_x + \cos x(\sin y\hat{\mathbf{e}}_y+\sin z\hat{\mathbf{e}}_z)]. \quad (2)$$

The velocity amplitude is chosen to be 2.5% of the Alfvén speed at tube center, i.e., $A_v=0.1$, which is equivalent to 4.25% of the sound speed outside the tubes. It should be emphasized that we do not impose any subsequent driver on the system, so that the flux tubes evolve freely. Uniform and isotropic resistivity (η) and viscosity (μ) are used, and are chosen so that the resistive and viscous Lundquist numbers ($S=V_AL_0/\eta$ and $S_v=V_AL_0/\mu$) are equal. In the above defi-

nitions, V_A is the initial Alfvén speed at the flux tube centers ($r=0$) and L_0 is a characteristic distance set equal to the initial flux tube radius. The two parameters that are varied in our system are the field line pitch or twist b, and the Lundquist number S. Low and high twist ($b=1$ and 10), and low and high Lundquist number ($S=576$ and 2880) runs have been performed.

RESULTS

Since the collision of orthogonal flux tubes is inherently 3D and nonlinear, there are no analytic solutions to this problem and, to our knowledge, this paper presents the first numerical simulations. From simulations of antiparallel magnetic flux tubes [14] and of orthogonal vortex tube interactions [18], we would expect the flux tubes to reconnect readily. The well-known ''slow'' reconnection models such as Sweet-Parker [9] and the tearing mode [7] yield a maximum reconnection velocity $V_r \sim S^{-1/2} V_A$. For our low Lundquist number case ($S=576$), we find that $V_r = 0.042 V_A$. In this case V_r exceeds the initial collision velocity so that the reconnection should easily be able to keep up with the motions. For the high Lundquist number case $V_r = 0.019 V_A$ and V_r is slightly less than the collision velocity. Of course, if ''fast'' Petschek reconnection [19] [$V_r \sim (\ln S) V_A$] occurs, then there should be no difficulty for the field lines to reconnect as fast as they are pushed together.

The arguments above lead us to conclude that for the low Lundquist number case, reconnection should dominate the collision process, so that two initially straight orthogonal tubes exchange halves to form two tubes bent at right angles. The bent tubes then straighten out and, thereby, decrease the total magnetic energy. In contrast to previous results, however, we find that for low twist, reconnection between the flux tubes is not substantial, even for low Lundquist numbers [20]. It should be emphasized that a simulation with identical parameters but with the flux tubes *antiparallel* resulted in the rapid merging of the tubes [21]. The evolution for *orthogonal* tubes, on the other hand, is primarily an elastic collision with little magnetic energy transfer to the plasma. This result is important to models of solar activity, because coronal flux tubes are believed to have low twist. Our results demonstrate that for small collision velocities, flux tube reconnection between initially orthogonal tubes is much more difficult to accomplish than is generally assumed. Unlike the situation of a neutral sheet, for example, reconnection does not occur spontaneously in orthogonal flux tubes. Of course, if the flux tubes are driven together by a continuously imposed velocity, they would necessarily reconnect. Also, if the initial collision velocity is much higher than the value we assumed, the reconnection would be more effective.

For the same initial velocity, we then attempted to obtain more reconnection by increasing the twist of the flux tubes to $b=10$ and by using a low Lundquist number ($S=576$). There are, at least, two reasons for expecting enhanced reconnection with higher twist. First, the magnetic energy of the Gold-Hoyle flux tubes in our model, see Eq. (1), decreases with larger twist. Hence, for the same collision velocity the deformation of the flux tubes increases. We note from Eq. (1) that at the flux tube axis the magnetic field strength is equal to B_0, independent of the twist, but at the tube boundary $B_R = B_0/\sqrt{1+b^2R^2}$. Thus the field strength at the boundary varies considerably with b. We find that $B_R/B_0 = 0.811$ for $b=1$ and $B_R/B_0 = 0.138$ for $b=10$. We can estimate the deformation of the flux tubes by equating the impulse exerted by the magnetic pressure at the flux tube boundary to the initial momentum of the tube. The momentum is given by $\rho(\pi R^2 L) V_c$, where $L = 2\pi$ is the tube length and V_c is the average collision velocity of the tube plasma. The impulse is given by the force exerted by the magnetic field of one flux tube on the other tube multiplied by the collision time τ_c. The force is given by $AB_R^2/8\pi$, where A is the area of contact of the two tubes. Let us assume that the collision causes a flattening of the tube so that the radius is decreased by a depth δ. Then $\tau_c \approx \delta/V_c$, and $A = \pi[R^2 - (R-\delta)^2] \approx 2R\delta$, where we assume that the contact area is circular and the deformation is small. Equating the momentum change to the impulse yields the following relation:

$$\frac{\delta}{R} = \frac{B_0}{B_R}\frac{V_c}{V_A}\left(\frac{L}{R}\right)^{1/2}. \tag{3}$$

We noted above that the maximum initial velocity is 2.5% V_A; hence taking the average collision velocity $V \approx 0.01 V_A$, we find from Eq. (3) that $\delta/R = 0.037$ for the low twist case and $\delta/R = 0.22$ for the high twist case. These results indicate that the tubes in the low twist case will undergo a minor deformation as a result of collision, but in the high twist case the deformation will be substantial, in fact, too large for the approximations used in deriving δ to remain valid. Therefore, reconnection should be much more pronounced in the high twist case.

Another reason for expecting enhanced reconnection in the high twist case is the coalescence instability. It is instructive to examine field line reconnection for the limiting cases of zero twist, so that all the field lines are initially straight, and for infinite twist, so that all the field lines are closed circles. As is sketched in Fig. 2(a), we expect reconnection between a straight vertical and a straight horizontal field line to result in two new field lines each of which is vertical along half its length and horizonal along the other half. These bent field lines will simply pull away from each other due to the magnetic tension at the bend and, thereby, create the so-called reconnection jets. Depending on how quickly the field lines move away, they may not hinder any subsequent reconnection at the collision point; on the other hand, they will not enhance it, either.

Now consider the reconnection of two circular field lines, one lying in a horizontal plane and the other in a vertical plane, Fig. 2(b). Reconnection results in a single new closed loop that is initially half vertical and half horizontal. In this case, magnetic tension produces three distinct effects. As before, reconnection jets form due to magnetic tension at the reconnection site. Another effect is that the new loop will tend to contract to a circular shape and thereby decrease its length. This is also analogous to the previous case. The reconnected line in 2(b) will tend to recover its original shape by ''circularizing,'' just as the reconnected lines in 2(a) will try to straighten out again. But now the contraction of the reconnected loop will cause more field lines to be

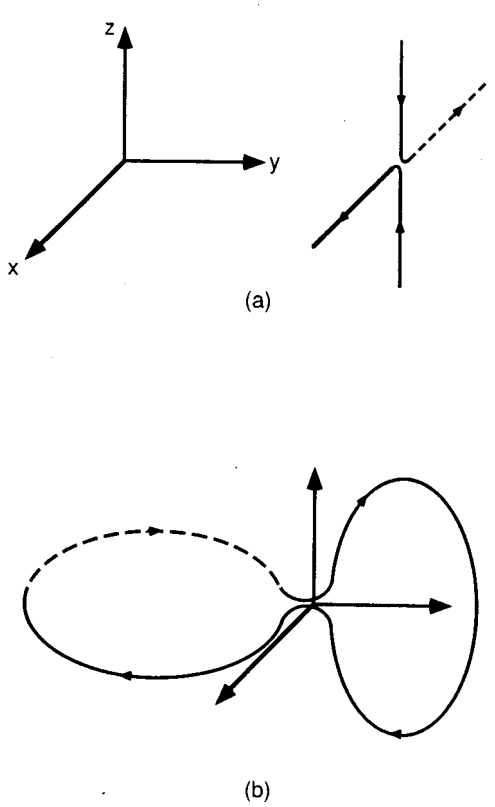

FIG. 2. (a) An illustration of two initially straight, orthogonal field lines that have just reconnected. (b) Two initially circular, orthogonal field lines that have just reconnected.

squeezed into the collision region and, thereby, will enhance subsequent reconnection. This process is simply the well-known coalescence instability. Increasing the twist of the flux tubes will increase the presence of the coalescence instability and will, therefore, enhance reconnection.

The third effect is not present in the straight field line case, and is due to the fact that the reconnected line in 2(b) is truly 3D and does not lie on a plane. One half is in a vertical plane and the other horizontal. Since the lowest energy state for a closed flux loop is a circle, the two halves will rotate so as to bring the loop onto a plane that is inclined at 45° to both the horizontal and vertical. The rotational motion can clearly be seen in the results presented below. Reconnected outer field lines exert a torque on the whole flux tube, causing both tubes to rotate by 45° and to line up in the collision region. To our knowledge, this rotation is a new effect that only appears in configurations like ours which involve nonplanar 3D flux tubes.

We find that the high-b, low-S case does, indeed, undergo much more reconnection than the low-b case. In fact, the evolution in this case closely resembles the standard vortex-tube reconnection picture described above—the initially straight tubes exchange halves to form two bent tubes [15,20]. We conclude that for sufficiently high twist and low Lundquist numbers, orthogonal flux tubes reconnect completely, just like antiparallel ones.

Since low Lundquist numbers generally are not relevant to space plasmas, however, we then considered the effect of increasing S.We speculated that, for sufficiently high S, the reconnection rate would decrease to the point that the tubes behave like the low twist case and simply bounce off each other. The actual evolution was a complete surprise—for $S=2880$ the tubes apparently pass right through each other.

We do not yet have a rigorous theory for this tunneling phenomenon, but it is straightforward to see how tunneling would occur if each field line undergoes a double reconnection process. Consider the two lines sketched in Fig. 3(a). The horizontal line is in the foreground and corresponds to an outer field line of the horizontal tube in our simulation, and the vertical line is in the background. Note that in addition to the bottom horizontal grid surface, we also show the two vertical side grid surfaces at $y=0$ and $y=2\pi$. Suppose that as a result of collision, the two lines are pressed against each other and that they reconnect twice, at diagonally opposite locations as shown in Fig. 3(b). By following any one

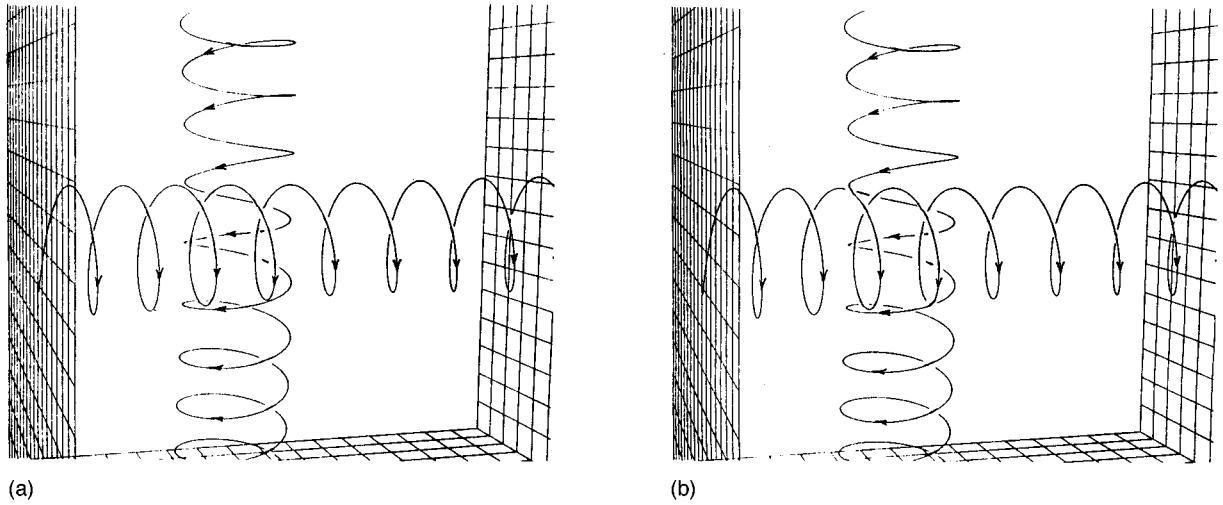

FIG. 3. (a) An illustration of two helical, orthogonal field lines before reconnection. The horizontal line is in the foreground, in front of the vertical line. (b) An illustration of the same field lines after two, diagonally opposite reconnections.

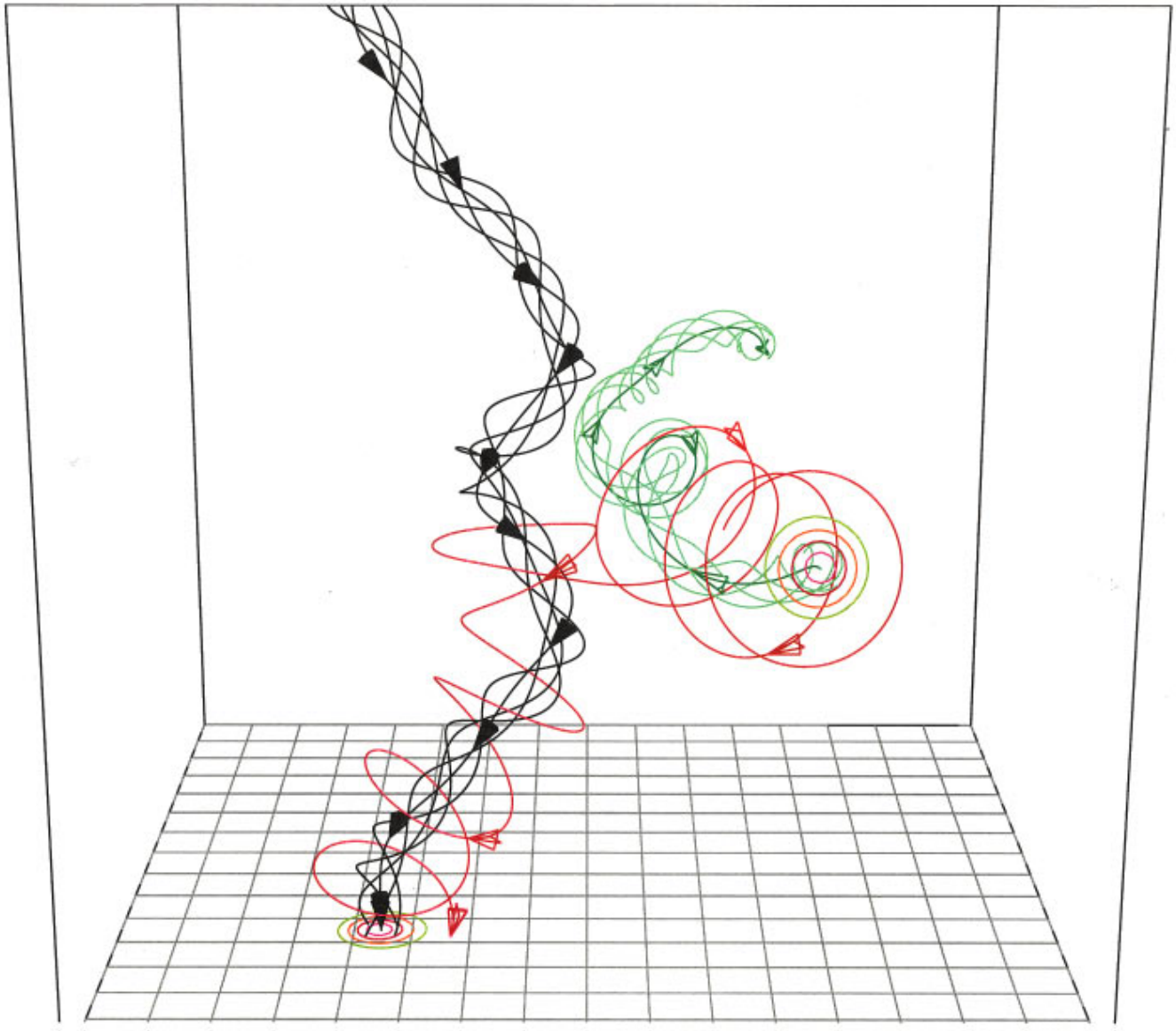

FIG. 4. (Color). A reconnected field line (red) at $t = 16.6$, that begins as a vertical twisted line, but then bends to become a horizontal line. All the other objects in the scene, including the viewpoint, have been selected as in Fig. 1. Note that the central field lines are beginning to exhibit a helical topology.

of the reconnected field lines, it can be seen that due to the reconnections, the tubes have exchanged their central sections so that now the vertical line passes in front of the horizontal one.

A close inspection of the field line connectivity in our numerical simulations supports this double reconnection model as the explanation for the tunneling. Figure 1 shows two representative outer field lines (red and blue) before reconnection. Figure 4 shows the effect of the reconnection of two such lines (for clarity only one of the reconnected field lines is shown). The lines exchange halves to form two right-angle lines, which are wrapped around both flux tubes and tend to pull the tubes together via the coalescence instability. Figure 5 shows the effects of the reconnection of two right-angle lines (again only one line is shown). We note that the vertical field line passes *around* the horizontal tube. A corresponding horizontal field line passes around the vertical tube. Such field lines are now free to continue on their initial trajectory without further interaction. This is the basic mechanism of magnetic tunneling: two reconnections at approximately fixed, diagonally opposite points in the collision region allow orthogonal field lines to exchange colliding sections and thereby pass through each other, as shown in Fig. 6.

The tunneling is most clearly seen in Fig. 7, which shows isosurfaces of the magnetic field magnitude at six times during the run. The isosurfaces are taken at half the maximum field magnitude value *at each time*. The viewpoint is along the x direction, so that the vertical flux tube is initially behind the horizontal flux tube. The effect of the first reconnections becomes clear as the reconnected field lines exert a torque on the tubes, as discussed above, causing them to

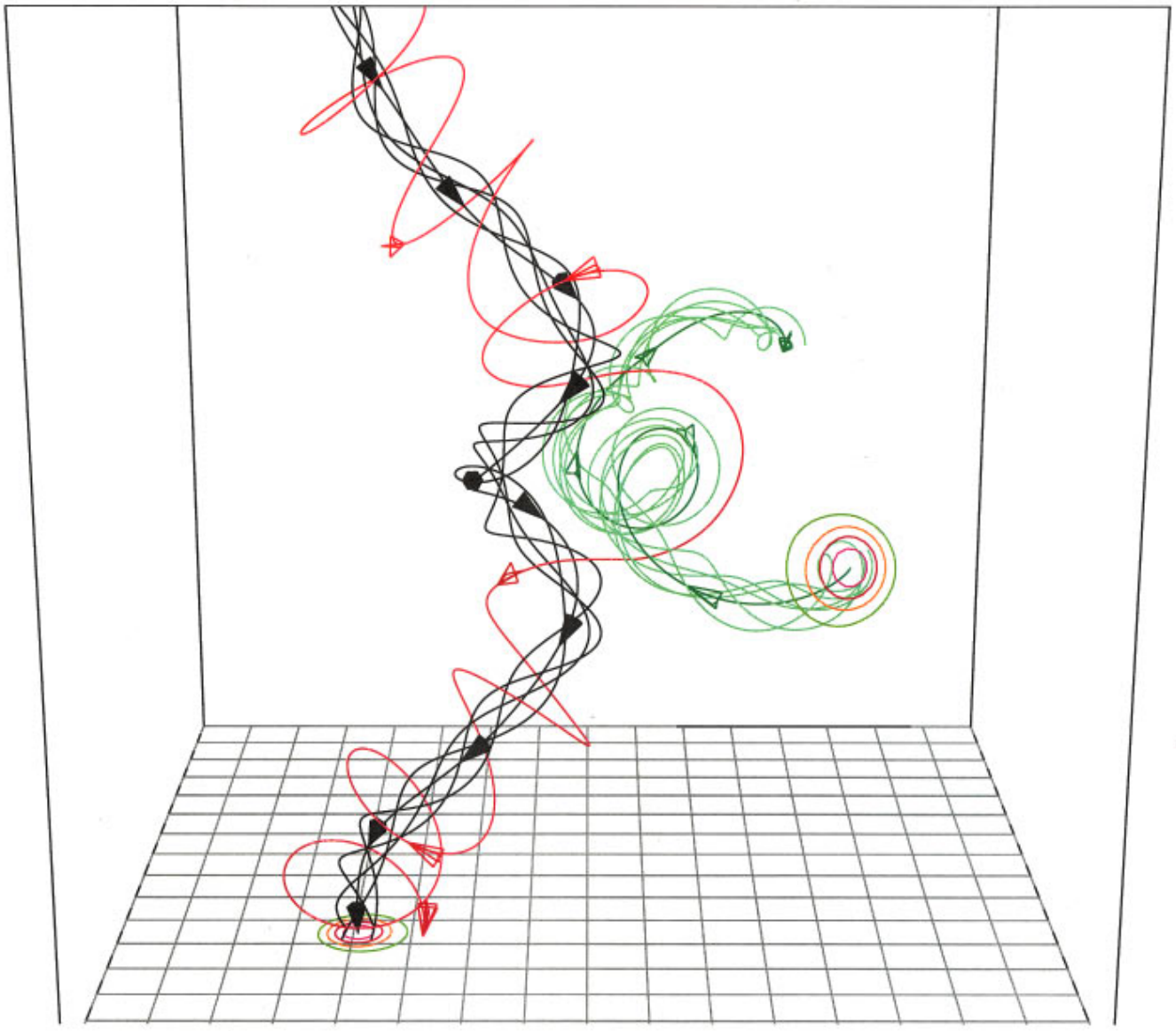

FIG. 5. (Color). A doubly reconnected field line (red) at $t=21.1$, that begins and ends as a vertical twisted line, but also wraps around the horizontal central line. All the other objects in the scene, including the viewpoint, have been selected as in Fig. 1. Note that the central field lines are almost intersecting.

rotate and become parallel in the interacting region. Initially, the singly reconnected field lines dominate, and the tubes begin to exchange halves. Then the doubly reconnected field dominates, with the central field lines pulling along the rest of the field lines. At the final time, the vertical tube is now in front of the horizontal tube, in complete contrast to the initial state.

The double reconnection explanation for the tunneling clearly requires a specific geometry for the reconnection region, in particular, the existence of two well-defined locations, where reconnection occurs or at least is strongly preferred. There are reasons to expect that such locations would arise naturally during the collision of the flux tubes in our model. Two areas can occur in the collision region where the opposing field lines from the two flux tubes are near antiparallel. It is evident from Fig. 1 that at the top of the horizontal tube, the blue field is oriented primarily toward the positive x direction, whereas at the near side of the vertical tube, the red field line is oriented toward the negative x direction. If the flux tubes wrap around each other sufficiently as they collide, one null area will be produced at the near upper corner of the collision region, along with a corresponding one in the far lower corner. It is widely believed that rapid reconnection is favored at magnetic null points [22]. In our case, it is not clear whether the field vanishes at isolated points in the collision region, or is simply much weaker at certain small areas. There is also the complication that since the initial field is confined to a finite volume of our system, null-field volumes are present throughout the simulation, so that conclusions based on analysis of isolated 3D null points may not apply.

We show in Fig. 8 one isosurface of strong electric cur-

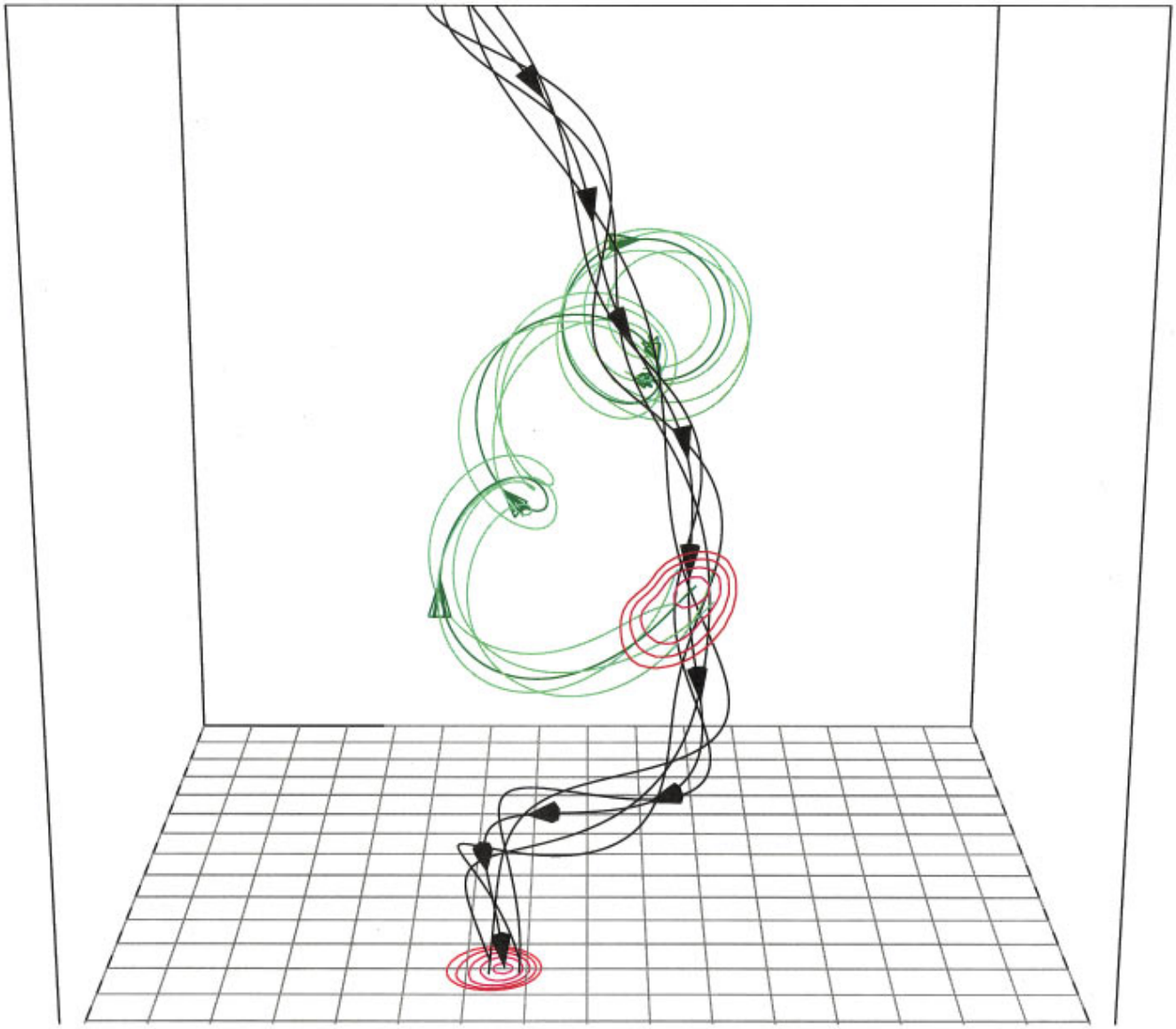

FIG. 6. (Color). Structure of the magnetic field at the end of the simulation ($t=82.5$), showing that the vertical flux tube now passes to the right of the horizontal one, and that the field lines have acquired a much more complex internal pattern than in Fig. 1. All the objects in the scene, including the viewpoint, have been selected as in Fig. 1.

rent density at a time during the simulation when reconnection is most dominant. Note that the current is concentrated in the collision region between the two flux tubes, and has a structure that runs from the upper corner to the lower corner, in agreement with the expected structure of the null areas. Reconnection should proceed faster at these areas if for no other reason than that the magnitude of the magnetic field component that changes sign is maximum here. Figure 8 again illustrates the difference between a truly 3D geometry and the usual configurations, such as 2D current sheets. In the 2D case the vanishing field component is constant over the reconnection region, whereas in a highly 3D current sheet the reconnection rate may vary strongly across the sheet, which could change the form of the whole reconnection process. This explains the dramatic difference between the evolution seen in the low S and high S cases. For high S the reconnection is confined to two spots, whereas for low S multiple reconnection occurs throughout the collision region so that the field can drop down to the lower-energy, bent flux tube state.

DISCUSSION

Several interesting issues and unanswered questions have been raised by our results. One important finding, evident in Figs. 6 and 7, is that the postreconnection flux tubes have very complex internal structure. In the initial Gold-Hoyle model, all field lines lie on well-defined cylindrical flux surfaces (Fig. 1), in fact, the Gold-Hoyle field is actually only one dimensional. Some of the initial twist of the flux tubes is lost during the double reconnection process—at least one winding. Since for high S magnetic helicity is expected to be approximately conserved [23], the helicity in the twist must transfer to internal wrappings of field lines about each other.

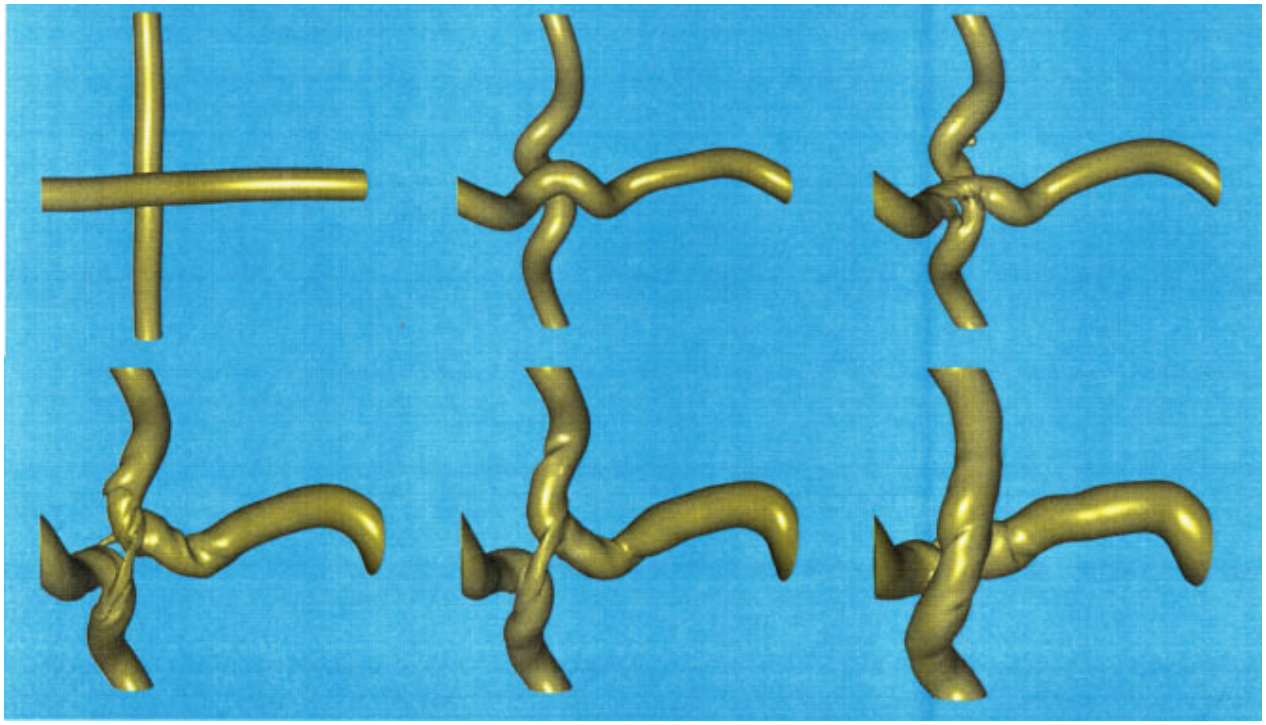

FIG. 7. (Color). Isosurfaces of $|\mathbf{B}|$at several times during the run. The left upper corner shows the result for $t=7.8$. To the right are the results for $t=21.1$ and 30.6. The left lower corner shows the result for $t=40.8$. To its right are the results for $t=52.2$ and 64.2. The isosurfaces are chosen to equal $|\mathbf{B}|_{\max}/2$ at each time.

We conclude that, as in the case of 2.5D studies [24], reconnection tends to produce a final field topology that is much more filamentary than the initial one. These results imply that magnetic flux tubes which erupt through the solar surface also are likely to have a fine-scale internal structure, which has important implications for coronal heating and activity [25].

An intriguing aspect of tunneling is the process by which the central field lines near the tube axis pass through each other. The double reconnection mechanism described above would seem to be inapplicable to them, since these field lines have vanishing twist. In fact, they also undergo a double reconnection similar to the highly twisted lines. Figure 7 shows that, during the height of the reconnection phase, both flux tubes are rotated so that they run diagonally through the reconnection sites. This rotation is due to field lines such as those in Fig. 4, which have already tunneled and exert a torque on the remaining field. The central field lines become parallel in the interaction region and are pulled toward the two reconnection regions by the coalescence effect, where they also reconnect and exchange central portions.

It should be noted that, for the high twist case, the energy in the azimuthal magnetic field $2\pi\int B_\phi^2 r\, dr$,is over three times the axial magnetic field energy. This is another reason for expecting tunneling to require a large twist. Unless the twist component dominates, it cannot deform the axial component sufficiently for that component also to undergo double reconnection. Due to the high twist, the kink instability also may be playing a role in the rotation of the axial magnetic field and its subsequent tunneling. Since the Gold-Hoyle model is metastable to first order, the kink mode growth rate is small [26], but it may be contributing to the helical deformation evident in Figs. 4–6. It would be instructive to repeat our simulations with a variety of initial flux tubes that have different distributions of axial and azimuthal field.

An interesting point to note is that the tunneling process may be nonreversible, because tubes prefer to tunnel in one direction only. This can be seen from Fig. 1. As stated in the Introduction, the tubes are positioned so as to maximize reconnection. On the side where they face each other the azimuthal component of the horizontal tube opposes the longitudinal component of the vertical tube and vice versa. Suppose the horizontal tube moves to the left and tunnels through, ending up to the left of the vertical tube. The relative orientation of the tubes is now different. If they collide again, the azimuthal component of the horizontal now reinforces the vertical longitudinal component. It may be that in this case the tubes cannot tunnel, but simply bounce. If so, it would imply that orthogonal flux tubes tend to have a preferred relative orientation. Simulations of collisions between flux tubes of different orientation are clearly needed in order to resolve this issue.

Another unanswered question is the importance of the symmetries in the system. The initial flux tubes are exactly orthogonal and have exactly the same flux and twist. We believe that the tunneling process described above should still occur for nonorthogonal, but large inclination, flux tubes and with differing magnetic structure, but this remains to be verified.

In the context of solar and space plasmas, the most important issue is the range of applicability of our results to the

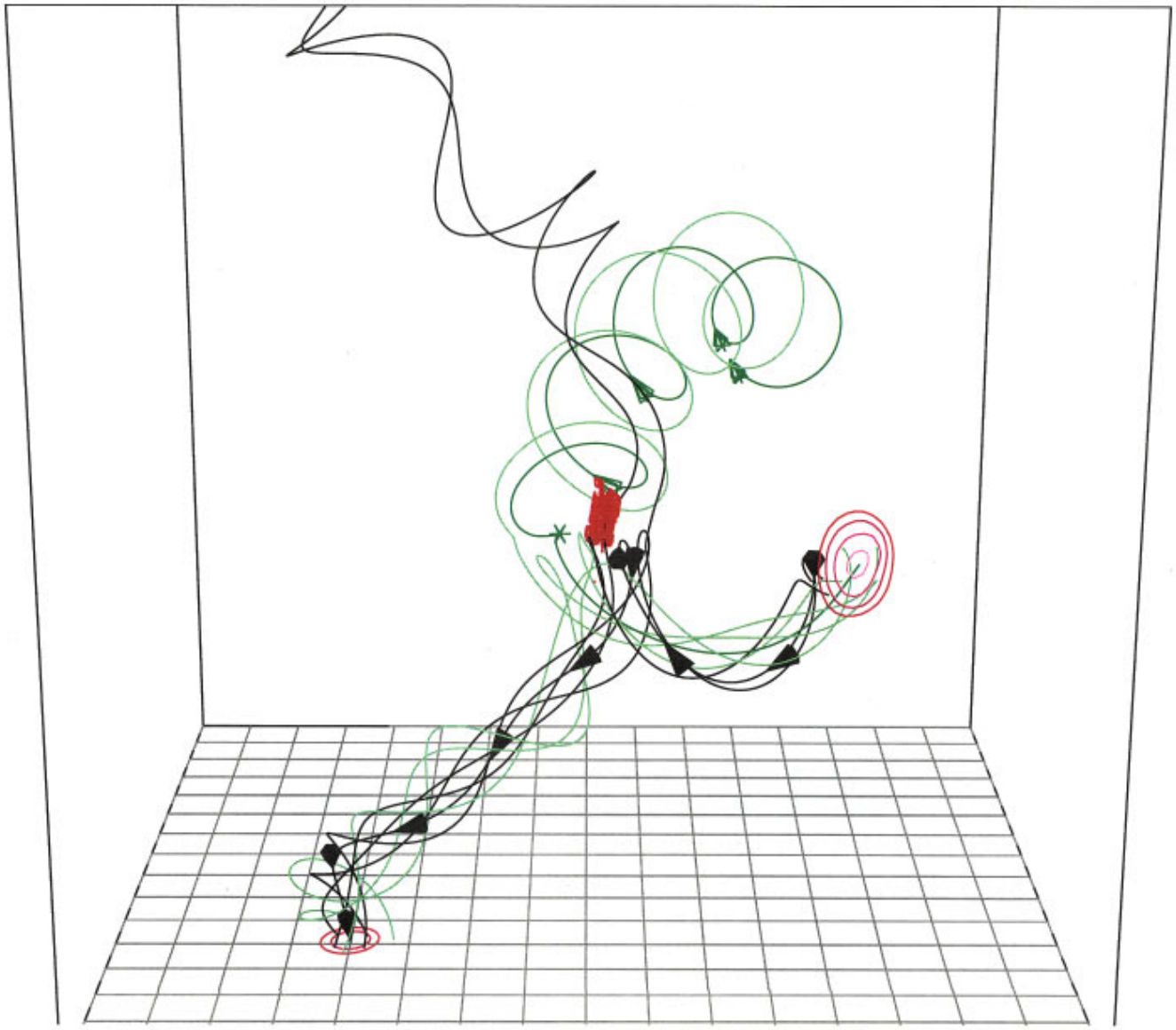

FIG. 8. (Color). Structure of the electric current density and magnetic field near the time of maximum flux tube interaction, $t=35.4$. Shown in red is the current magnitude isosurface at 75% of maximum. The field lines in the scene have been selected as in Fig. 1, but for better viewing of the current structure, the scene has been rotated by 90° from that in Fig. 1, so that x is into the figure and the viewer is directly behind the collision region. Note that the tubes are completely entangled at this time and that the current structure runs from the upper right to lower left diagonal.

very large Lundquist number regime. We have two main conclusions—for modest collision velocities, low twist orthogonal tubes bounce and high twist tubes tunnel. The first result should be even more valid at higher S; hence, flux tube reconnection is unlikely to be common in the solar corona unless the tubes are driven together, or are nearly antiparallel. We believe that the second result also holds for higher S because as long as the expected deformation is large, the rate of reconnection depends weakly on S, but this is only a conjecture.

It is clear that the work described above has produced numerous questions requiring further numerical and theoretical work. It may even be possible to reproduce some of the results in the laboratory. We look forward to many future investigations on this curious phenomenon of flux tube tunneling.

ACKNOWLEDGMENTS

We thank Dr. A. B. Hassam and Dr. E. R. Priest for helpful conversations. We also thank Dr. J. T. Karpen and Dr. J. A. Klimchuk for commenting on the manuscript. This work was sponsored by the NASA High Performance Computing and Communications Program, the NASA Space Physics Theory Program, and ONR. The computations were performed on the Naval Research Laboratory CM5E under a grant of time from the DoD HPC program.

[1] E. N. Frazier and J. O. Stenflo, Solar Phys. **27**, 330 (1972).
[2] P. A. Sturrock and Y. Uchida, Astrophys. J. **246**, 331 (1981).
[3] J. T. Karpen, S. K. Antiochos, R. B. Dahlburg, and D. S. Spicer, Astrophys. J. **403**, 769 (1993).
[4] E. N. Parker, Astrophys. J. **264**, 642 (1983).
[5] E. N. Parker, Astrophys. J. **330**, 474 (1988).
[6] G. Roumeliotis, Astrophys. J. **379**, 392 (1991).
[7] P. A. Sturrock, P. Kaufman, R. L. Moore, and D. F. Smith, Solar Phys. **94**, 341 (1984).
[8] M. E. Machado, K. K. Ong, A. G. Emslie, G. Fishman, C. Meegan, R. B. Wilson, and W. S. Paciesas, Adv. Space Res. **13**, 175 (1993).
[9] E. G. Zweibel and J. E. Rhoads, Astrophys. J. **440**, 407 (1995).
[10] L. W. Klein and L. F. Burlaga, J. Geophys. Res. **87**, 613 (1982).
[11] B. U. O. Sonnerup *et al.*, J. Geophys. Res. **86**, 10049 (1981).
[12] J. Birn and E. W. Hones, Jr., J. Geophys. Res. **86**, 6802 (1981).
[13] R. B. Dahlburg and J. M. Picone, Phys. Fluids B **1**, 2153 (1989).
[14] R. B. Dahlburg and S. K. Antiochos, J. Geophys. Res. **100**, 16991 (1995).
[15] R. B. Dahlburg and D. Norton, in *Small Scale Structures in Three Dimensional Hydrodynamic and Magnetohydrodynamic Turbulence*, edited by M. Meneguzzi, A. Pouquet, and P.-L. Sulem (Springer-Verlag, Heidelberg, 1995), p. 331.
[16] T. Gold and F. Hoyle, Mon. Not. R. Astron. Soc. **120**, 89 (1958).
[17] C. Canuto, M. Y. Hussaini, A. Quarteroni, and T. A. Zang, *Spectral Methods in Fluid Mechanics* (Springer-Verlag, New York, 1987).
[18] O. N. Boratav, R. B. Pelz, and N. J. Zabusky, Phys. Fluids A **4**, 581 (1992).
[19] M. Jardine, J. Plasma Phys. **51**, 399 (1994).
[20] R. B. Dahlburg and S. K. Antiochos, Adv. Space Res. **19**, 1781 (1997).
[21] R. B. Dahlburg and S. K. Antiochos, EOS **77**, 210 (1996).
[22] J. M. Greene, J. Geophys. Res. **93**, 8583 (1988).
[23] J. B. Taylor, Phys. Rev. Lett. **33**, 11398 (1974).
[24] J. T. Karpen, S. K. Antiochos, and C. R. DeVore, Astrophys. J. **460**, L73 (1996).
[25] P. L. Similon and R. N. Sudan, Astrophys. J. **336**, 442 (1989).
[26] M. G. Linton, D. W. Longcope, and G. H. Fisher, Astrophys. J. **469**, 954 (1995).